INTERNATIONAL JOURNAL FOR NUMERICAL METHODS IN FLUIDS
Int. J. Numer. Meth. Fluids **31**: 1265–1280 (1999)

COMPARISON OF USING CARTESIAN AND COVARIANT VELOCITY COMPONENTS ON NON-ORTHOGONAL COLLOCATED GRIDS

YUNLIANG WANG* AND SATORU KOMORI

Department of Mechanical Engineering, Kyoto University, Kyoto 606-8501, Japan

SUMMARY

In this paper, the Cartesian velocity components and the covariant velocity components are adopted respectively as the main variables in solving the momentum equations in the SIMPLE-like method to calculate a lid-driven cavity flow on non-orthogonal collocated grids. In total, more than 400 computer runs are carried out for a two-dimensional problem. The accuracy and convergence performance of using Cartesian and covariant velocity components are compared in detail. Comparisons show that both the Cartesian and covariant velocity methods have the same numerical accuracy. The convergence rate of the covariant velocity method can be faster than that of the Cartesian velocity method if the relaxation factor for pressure is small enough. However, the convergence range of the relaxation factor for pressure in the covariant velocity method is quite narrow. When the cross-derivatives in the pressure-correction equation are retained approximately, its convergence performance can be greatly improved. Copyright © 1999 John Wiley & Sons, Ltd.

KEY WORDS: cavity flow; SIMPLE method; covariant velocity; non-orthogonal grid; collocated grid

1. INTRODUCTION

Since the appearance of the SIMPLE method [1], wide use has been made of it in the numerical computation of incompressible flows. In order to improve the convergence performance of the SIMPLE method, various variants have been developed, such as the SIMPLER [2] and SIMPLEC [3] methods. Originally, the SIMPLE method used a staggered grid system to avoid the appearance of the checkerboard pressure field. Owing to the difficulty of programme making on a staggered grid system, people had been trying to solve the pressure oscillation problem on a collocated grid system. Rhie and Chow [4] first successfully solved the pressure oscillation problem on a collocated grid by using the cell-face momentum interpolation technique. Peric *et al.* [5] and Melaaen [6,7] compared the accuracy and convergence performance of the staggered and collocated grid methods on orthogonal and non-orthogonal grids. Their comparisons show that there is no significant difference between the two grid systems. Therefore, more and more studies based on the collocated grid system have appeared owing to its simplicity [8–10].

* Correspondence to: Department of Mechanical Engineering, Kyoto University, Kyoto 606-8501, Japan. Fax: +81 75 7535245; e-mail: ylwang@mech.kyoto-u.ac.jp

CCC 0271–2091/99/241265–16$17.50

Received August 1998
Revised November 1998

For computations of fluid flow on the orthogonal grid, there is no difficulty for the SIMPLE-like method to reach a convergent solution. When the grids are strongly non-orthogonal, however, a convergence difficulty is frequently encountered. For example, Peric [9] had to use a relaxation factor for pressure as low as 0.05 to get a convergent solution for the flow in a curved channel. Ricon and Elder [10] also had to adopt a relaxation factor for pressure as low as 0.05 to calculate the flow through turbine cascades.

For non-orthogonal grids there are several ways to select the main variables in solving the momentum equations, such as the Cartesian, covariant and contravariant velocity components. Usually, the Cartesian velocity components are used as the main variables in the momentum equations (the so-called Cartesian velocity method). When the covariant velocity components are regarded as the main variables, the pressure–velocity coupling can become quite simple, and the numerical error to calculate the cross-derivatives of the pressure gradient can be avoided (the so-called covariant velocity method). However, the expression of convective and diffusive fluxes is more complicated. When the Cartesian velocity method is used on strongly non-orthogonal grids, the staggered grid system is invalid in avoiding the checkerboard pressure field, since the directions of the grid lines are no longer the same as those of the Cartesian velocity components. For the staggered grid system, therefore, the covariant or contravariant velocity method is the better choice for avoiding the checkerboard pressure field. For the collocated grid system, one can avoid the checkerboard pressure field using the cell face momentum interpolation scheme regardless if the Cartesian, covariant or contravariant velocity components are adopted. For the convenience of programming, the covariant method is frequently used on a collocated grid system. For example, Karki and Patankar [11] adopted the covariant velocity method on a staggered grid system. Demirdzic *et al.* [12], Tamamidis and Assanis [13] and Wang and Komori [14] adopted the covariant velocity method on a collocated grid system. However, nobody has proven whether the convergence performance of the covariant velocity method is really superior to that of the Cartesian velocity method in the SIMPLE-like method. In this paper, the numerical accuracy and convergence performance of the Cartesian and covariant velocity methods are compared by solving a two-dimensional lid-driven cavity flow on non-orthogonal collocated grids. Some valuable conclusions are drawn from the comparisons.

2. MATHEMATICAL FORMULATION

2.1. Governing equations

The continuity equation and the conservation form of the transport equation for a general dependent variable ϕ in a curvilinear co-ordinate system (ξ, η) can be written as

$$\frac{\partial}{\partial \xi}(\rho U) + \frac{\partial}{\partial \eta}(\rho V) = 0, \tag{1}$$

$$\frac{\partial}{\partial \xi}(\rho U \phi) + \frac{\partial}{\partial \eta}(\rho V \phi) = \frac{\partial}{\partial \xi}\left[\frac{\Gamma}{J}(\varphi \phi_\xi - \chi \phi_\eta)\right] + \frac{\partial}{\partial \eta}\left[\frac{\Gamma}{J}(\gamma \phi_\eta - \chi \phi_\xi)\right] + JS(\xi, \eta), \tag{2}$$

where U and V are the contravariant velocity components; Γ is the general diffusion coefficient, and J is the Jacobian of the transformation; $S(\xi, \eta)$ is the source term on the computational plane; with χ, φ and γ as the coefficients of transformation.

$$U = uy_\eta - vx_\eta, \qquad V = vx_\xi - uy_\xi, \tag{3}$$

$$J = x_\xi y_\eta - x_\eta y_\zeta, \qquad \chi = x_\xi x_\eta + y_\xi y_\eta, \tag{4a}$$

$$\varphi = x_\eta^2 + y_\eta^2, \qquad \gamma = x_\xi^2 + y_\xi^2. \tag{4b}$$

2.2. Discretization of the transport equation

Integrating Equation (2) over the control volume of node P as shown in Figure 1, you get

$$[\rho U\phi]_{\mathrm{w}}^{\mathrm{e}} + [\rho V\phi]_{\mathrm{s}}^{\mathrm{n}} = \left[\frac{\Gamma}{J}(\varphi\phi_\xi - \chi\phi_\eta)\,\Delta\eta\right]_{\mathrm{w}}^{\mathrm{e}} + \left[\frac{\Gamma}{J}(\gamma\phi_\eta - \chi\phi_\xi)\,\Delta\xi\right]_{\mathrm{s}}^{\mathrm{n}} + JS(\xi,\eta)\,\Delta\xi\,\Delta\eta. \tag{5}$$

When a proper scheme is used to calculate the convection and diffusion terms in Equation (5), the finite difference equation can be written as

$$A_P\phi_P = A_{\mathrm{E}}\phi_{\mathrm{E}} + A_{\mathrm{W}}\phi_{\mathrm{W}} + A_{\mathrm{N}}\phi_{\mathrm{N}} + A_{\mathrm{S}}\phi_{\mathrm{S}} + S_{\mathrm{NEW}}. \tag{6}$$

In this study, the power-law scheme is used.

Usually, all variables are underrelaxed in iteration so as to guarantee the convergence of the solution. As a result, Equation (6) can be rewritten as

$$\frac{A_P}{\alpha}\phi_P = \sum A_{\mathrm{nb}}\phi_{\mathrm{nb}} + S_{\mathrm{NEW}} + (1-\alpha)\frac{A_P}{\alpha}\phi_P^*, \tag{7}$$

where α is the relaxation factor. The superscript asterisk denotes the value of the last iteration.

Equation (7) is the general form for all dependent variables. For the Cartesian velocity components u and v, Equation (7) can be rearranged as

$$\frac{A_P}{\alpha_u}u_P = \sum A_{\mathrm{nb}}u_{\mathrm{nb}} + S_u + \frac{(1-\alpha_u)}{\alpha_u}A_P u_P^*, \tag{8a}$$

$$\frac{A_P}{\alpha_u}v_P = \sum A_{\mathrm{nb}}v_{\mathrm{nb}} + S_v + \frac{(1-\alpha_u)}{\alpha_u}A_P v_P^*, \tag{8b}$$

where α_u is the relaxation factor for velocity. S_u and S_v are the corresponding source terms.

When the pressure gradient terms are separated from the source terms, Equations (8a) and (8b) can be rewritten as

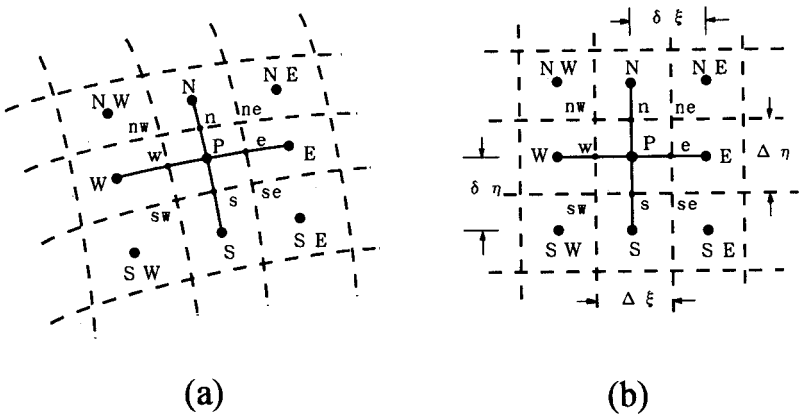

Figure 1. Grid arrangements: (a) physical plane; (b) computational plane.

$$\frac{A_P}{\alpha_u} u_P = \sum A_{\mathrm{nb}} u_{\mathrm{nb}} + S_u - (y_\eta p_\xi - y_\xi p_\eta)\,\Delta\xi\,\Delta\eta + \frac{(1-\alpha_u)}{\alpha_u} A_P u_P^*, \tag{9a}$$

$$\frac{A_P}{\alpha_u} v_P = \sum A_{\mathrm{nb}} v_{\mathrm{nb}} + S_v - (x_\xi p_\eta - x_\eta p_\xi)\,\Delta\xi\,\Delta\eta + \frac{(1-\alpha_u)}{\alpha_u} A_P v_P^*. \tag{9b}$$

When the Cartesian velocity components are adopted as the main variables in the momentum equations, Equations (9a) and (9b) can be solved for u and v. However, when the covariant velocity components u_ξ and u_η are used as the main variables, discretization equations for u_ξ and u_η should be derived. These discretization equations can be derived using the conventional differential formulation approach. To avoid the use of tensor analysis for the derivation of the curvature source terms, however, discretization equations for u_ξ and u_η are usually obtained in the algebraic way [11,13,14].

The covariant velocity components u_ξ and u_η are related to u and v via

$$u_\xi = (u x_\xi + v y_\xi)/\gamma^{1/2}, \tag{10a}$$

$$u_\eta = (u x_\eta + v y_\eta)/\varphi^{1/2}. \tag{10b}$$

Substitution of Equations (9a) and (9b) into Equation (10a), for example, yields

$$\frac{A_P}{\alpha_u} u_{\xi,P} = \sum A_{\mathrm{nb}} u'_{\xi,\mathrm{nb}} + S'_{u_\xi} + \frac{(1-\alpha_u)}{\alpha_u} A_P u^*_{\xi,P}, \tag{11}$$

where

$$u'_{\xi,\mathrm{nb}} = (x_\xi/\gamma^{1/2})_P u_{\mathrm{nb}} + (y_\xi/\gamma^{1/2})_P v_{\mathrm{nb}}, \tag{12}$$

$$S'_{u_\xi} = (x_\xi/\gamma^{1/2})_P S_u + (y_\xi/\gamma^{1/2})_P S_v. \tag{13}$$

Rearranging Equation (11), the discretization equation for u_ξ can be derived as

$$\frac{A_P}{\alpha_u} u_{\xi,P} = \sum A_{\mathrm{nb}} u_{\xi,\mathrm{nb}} + \sum A_{\mathrm{nb}} (u'_{\xi,\mathrm{nb}} - u^*_{\xi,\mathrm{nb}}) + S'_{u_\xi} + \frac{(1-\alpha_u)}{\alpha_u} A_P u^*_{\xi,P}. \tag{14}$$

For later reference, Equation (14) can be rewritten in a compact form, with the pressure gradient term appearing explicitly on the right-hand side:

$$\frac{A_P}{\alpha_u} u_{\xi,P} = \sum A_{\mathrm{nb}} u_{\xi,\mathrm{nb}} - p_\xi c_\xi + S_{u_\xi} + \frac{(1-\alpha_u)}{\alpha_u} A_P u^*_{\xi,P}, \tag{15a}$$

where $c_\xi = J\,\Delta\xi\,\Delta\eta/\gamma^{1/2}$. S_{u_ξ} is the source term excluding the pressure gradient term.

Similarly, the discretization equation for u_η can be written as

$$\frac{A_P}{\alpha_u} u_{\eta,P} = \sum A_{\mathrm{nb}} u_{\eta,\mathrm{nb}} - p_\eta c_\eta + S_{u_\eta} + \frac{(1-\alpha_u)}{\alpha_u} A_P u^*_{\eta,P}, \tag{15b}$$

where $c_\eta = J\,\Delta\xi\,\Delta\eta/\varphi^{1/2}$. S_{u_η} is the source term excluding the pressure gradient term.

Compared with Equations (9a) and (9b), it is seen that the cross-derivatives of pressure in Equations (15a) and (15b) have disappeared. Therefore, in the covariant velocity method, the pressure–velocity coupling will become easier.

2.3. Pressure-correction equation

In the SIMPLE-like method, pressure is calculated using the correction method. The pressure-correction equation can be derived from the continuity equation. When the momentum equations have been solved, the Cartesian, covariant, contravariant velocity components

and pressure are supposed to be u^*, v^*, u^*_ξ, u^*_η, U^*, V^* and p^*, which in general do not satisfy the continuity equation. To satisfy the continuity equation, the corresponding corrections are supposed to be u', v', u'_ξ, u'_η, U', V' and p'. Therefore, there exists the following relations:

$$u = u^* + u', \qquad v = v^* + v', \tag{16a}$$

$$u_\xi = u^*_\xi + u'_\xi, \qquad u_\eta = u^*_\eta + u'_\eta, \tag{16b}$$

$$U = U^* + U', \qquad V = V^* + V', \tag{16c}$$

$$p = p^* + p'. \tag{16d}$$

Substituting Equations (16a) and (16d) into Equations (9a) and (9b), you get

$$\frac{A_P}{\alpha_u} u'_P = \sum A_{\mathrm{nb}} u'_{\mathrm{nb}} - (y_\eta p'_\xi - y_\xi p'_\eta)\,\Delta\xi\,\Delta\eta, \tag{17a}$$

$$\frac{A_P}{\alpha_u} v'_P = \sum A_{\mathrm{nb}} v'_{\mathrm{nb}} - (x_\xi p'_\eta - x_\eta p'_\xi)\,\Delta\xi\,\Delta\eta. \tag{17b}$$

From previous experience, it is found that when the SIMPLEC method is used to approximate the pressure–velocity coupling, the convergence performance on strongly non-orthogonal grids can be greatly improved in comparison with the SIMPLE method. Therefore, the SIMPLEC method is also adopted in this study. According to the SIMPLEC method, the relations between velocity corrections and pressure corrections can be written as

$$u'_P = (B^u p'_\xi + C^u p'_\eta), \tag{18a}$$

$$v'_P = (B^v p'_\xi + C^v p'_\eta), \tag{18b}$$

where

$$B^u = -\frac{y_\eta\,\Delta\xi\,\Delta\eta}{A_P/\alpha_u - \sum A_{\mathrm{nb}}}, \qquad C^u = -\frac{y_\xi\,\Delta\xi\,\Delta\eta}{A_P/\alpha_u - \sum A_{\mathrm{nb}}}, \tag{19a}$$

$$B^v = \frac{x_\eta\,\Delta\xi\,\Delta\eta}{A_P/\alpha_u - \sum A_{\mathrm{nb}}}, \qquad C^v = -\frac{x_\xi\,\Delta\xi\,\Delta\eta}{A_P/\alpha_u - \sum A_{\mathrm{nb}}}. \tag{19b}$$

By substituting Equations (18a) and (18b) into Equation (3), corrections of the contravariant velocity components can be written as

$$U' = (B^u y_\eta - B^v x_\eta)p'_\xi + \underline{(C^u y_\eta - C^v x_\eta)p'_\eta}, \tag{20a}$$

$$V' = (C^v x_\xi - C^u y_\xi)p'_\eta + \underline{(B^v x_\xi - B^u y_\xi)p'_\xi}, \tag{20b}$$

where the underlined parts in Equations (20a) and (20b) are usually called the cross-derivatives of the pressure corrections, and for orthogonal grids they are zero.

In the covariant velocity method, corrections of the covariant velocity components can be calculated by

$$u'_\xi = -\frac{p'_\xi c_\xi}{A_P/\alpha_u - \sum A_{\mathrm{nb}}}, \tag{21a}$$

$$u'_\eta = -\frac{p'_\eta c_\eta}{A_P/\alpha_u - \sum A_{\mathrm{nb}}}. \tag{21b}$$

According to the definition of the contravariant velocity components, the corrections of the contravariant velocity components are related to the corrections of the covariant velocity components via

$$U' = (\varphi\gamma^{1/2}u'_\xi - \chi\varphi^{1/2}u'_\eta)/J, \tag{22a}$$

$$V' = (\gamma\varphi^{1/2}u'_\eta - \chi\gamma^{1/2}u'_\xi)/J. \tag{22b}$$

If Equations (21a) and (21b) are substituted into Equations (22a) and (22b), Equations (20a) and (20b) can also be derived. Therefore, no matter if the covariant velocity components or the Cartesian velocity components are adopted as the main variables in the momentum equations, the relations between the corrections of the contravariant velocity components and pressure corrections are identical.

Then the contravariant velocity components satisfying the continuity equation can be expressed as

$$U = U^* + Bp'_\xi + Dp'_\eta, \tag{23a}$$

$$V = V^* + Cp'_\eta + Ep'_\xi, \tag{23b}$$

where

$$B = B^u y_\eta - B^v x_\eta, \qquad C = C^v x_\xi - C^u y_\xi, \tag{24a}$$

$$D = (C^u y_\eta - C^v x_\eta), \qquad E = (B^v x_\xi - B^u y_\xi). \tag{24b}$$

When Equation (1) is integrated over the control volume of node P, the discretization form of the continuity equation can be written as

$$[\rho U\,\Delta\eta]_{\mathrm{w}}^{\mathrm{e}} + [\rho V\,\Delta\xi]_{\mathrm{s}}^{\mathrm{n}} = 0. \tag{25}$$

Substituting Equations (23a) and (23b) into Equation (25), and neglecting the cross-derivatives of pressure corrections, the pressure-correction equation can be formulated as

$$A_P^p p'_P = A_{\mathrm{E}}^p p'_{\mathrm{E}} + A_{\mathrm{W}}^p p'_{\mathrm{W}} + A_{\mathrm{N}}^p p'_{\mathrm{N}} + A_{\mathrm{S}}^p p'_{\mathrm{S}} + m_p, \tag{26}$$

where

$$A_{\mathrm{E}}^p = (\rho B\,\Delta\eta/\delta\xi)_{\mathrm{e}}, \tag{27a}$$

$$A_{\mathrm{W}}^p = (\rho B\,\Delta\eta/\delta\xi)_{\mathrm{w}}, \tag{27b}$$

$$A_{\mathrm{N}}^p = (\rho C\,\Delta\xi/\delta\eta)_{\mathrm{n}}, \tag{27c}$$

$$A_{\mathrm{S}}^p = (\rho C\,\Delta\xi/\delta\eta)_{\mathrm{s}}, \tag{27d}$$

$$A_P^p = A_{\mathrm{E}}^p + A_{\mathrm{W}}^p + A_{\mathrm{N}}^p + A_{\mathrm{S}}^p, \tag{27e}$$

$$m_p = (\rho U^*\Delta\eta)_{\mathrm{e}} - (\rho U^*\Delta\eta)_{\mathrm{w}} + (\rho V^*\Delta\xi)_{\mathrm{n}} - (\rho V^*\Delta\xi)_{\mathrm{s}}. \tag{27f}$$

When the pressure-correction has been solved, Equations (21a) and (21b) are used to calculate the corrections of the covariant velocity components in the covariant velocity method. However, in the Cartesian velocity method, Equations (20a) and (20b), neglecting the cross-derivatives of the pressure corrections, are used to calculate the corrections of the contravariant velocity components. Then the following relations are used to calculate the corrections of the Cartesian velocity components:

$$u' = (U'x_\xi + V'x_\eta)/J, \tag{28a}$$

$$v' = (U'y_\xi + V'y_\eta)/J. \tag{28b}$$

2.4. Momentum interpolation technique

On a collocated grid system, the checkerboard pressure field will be encountered unless some special treatments are taken. Rhie and Chow [4] first developed the following cell-face momentum interpolation technique to overcome this problem:

$$U_e^* = \bar{U}_e^* + \left(\frac{\varphi}{A_P/\alpha_u}\right)_e \left[\left(\overline{\frac{\partial p^*}{\partial \xi}}\right)_e - \left(\frac{\partial p^*}{\partial \xi}\right)_e\right], \tag{29}$$

where the overbar implies that values are obtained by a linear interpolation scheme.

It is seen that α_u is included in Equation (29). Majumdar [15] has found that with the use of Equation (29), the final convergent result will depend on α_u. In order to get a convergent solution independent of the relaxation factor used for velocity, the following formula is adopted:

$$U_e^* = \bar{U}_e^* + \left(\frac{\varphi}{A_P}\right)_e \left[\left(\overline{\frac{\partial p^*}{\partial \xi}}\right)_e - \left(\frac{\partial p^*}{\partial \xi}\right)_e\right]. \tag{30a}$$

Similarly, the contravariant velocity V^* at cell-face n can be calculated by

$$V_n^* = \bar{V}_n^* + \left(\frac{\gamma}{A_P}\right)_n \left[\left(\overline{\frac{\partial p^*}{\partial \eta}}\right)_n - \left(\frac{\partial p^*}{\partial \eta}\right)_n\right]. \tag{30b}$$

Equations (30a) and (30b) were always used by Melaaen [6,7].

2.5. Solution algorithm

The overall solution algorithm is as follows:

1. Guess values for all the variables.
2. In the Cartesian velocity method, solve Equations (9a) and (9b) to obtain u^* and v^*. In the covariant velocity method, solve Equations (15a) and (15b) to obtain u_ξ^* and u_η^*.
3. Calculate the contravariant velocity components at cell-faces using Equations (30a) and (30b), and thereby calculate the source term of the pressure-correction equation.
4. Solve the pressure-correction equation, i.e. Equation (26), to obtain p'.
5. Use the pressure corrections to correct the pressure field via

$$p = p^* + \alpha_p p', \tag{31}$$

   where α_p is the relaxation factor for pressure.
6. Correct the contravariant velocity components using Equations (20a) and (20b), neglecting the cross-derivatives of the pressure corrections.
7. In the Cartesian velocity method, correct the Cartesian velocity components using Equations (28a) and (28b). In the covariant velocity method, correct the covariant velocity components using Equations (21a) and (21b).
8. Return to step (2) and repeat the whole procedure until a convergent solution is achieved.

3. RESULTS AND DISCUSSIONS

The laminar flow in a cavity with a moving lid, as shown in Figure 2, is often used as a test to validate a numerical procedure. In this study, the Reynolds numbers based on the velocity of the moving lid and the side length of the cavity are 100 and 1000 respectively. The inclined angle between two sides of the cavity is changed from 90° to 30°. In total, four cases, i.e. $\beta = 30°$, 45°, 60° and 90° are investigated using the Cartesian and covariant velocity methods.

3.1. Accuracy

In order to validate the numerical accuracy of the present procedure, it is first applied to calculate the 90° cavity flow with a Reynolds number of 100. The profiles of velocities in the x- and y-directions are compared with the benchmark data of Ghia *et al.* (1982) [16]. The computed profiles of velocity U at $x = L/2$ with three kinds of uniform grid are shown in

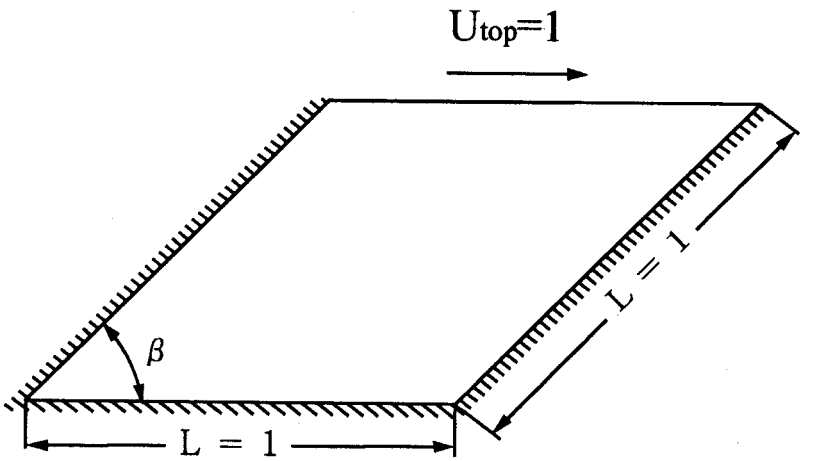

Figure 2. Cavity geometry and boundary condition.

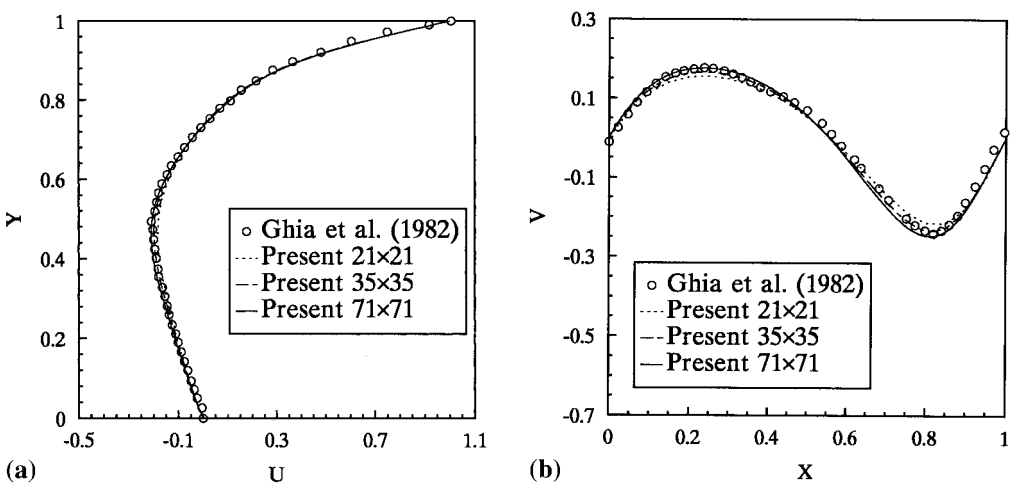

Figure 3. Profiles of velocities for a cavity at $\beta = 90°$, $Re = 100$: (a) U; (b) V.

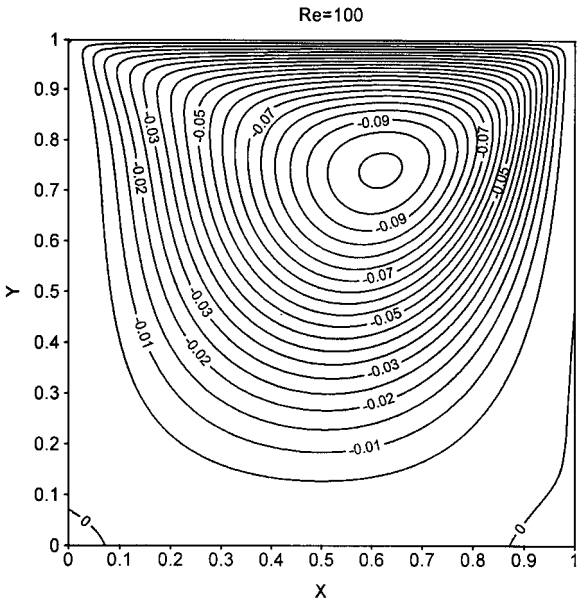

Figure 4. Calculated streamlines for a cavity at $\beta = 90°$.

Figure 3(a). The convergence criterion is that the maximum residual in the pressure-correction equation falls below 10^{-8}.

The corresponding computed profiles of velocity V at $y = L/2$ are shown in Figure 3(b). From Figure 3(a) and (b) it is seen that with increasing grid points, the computed profiles of both U and V become closer to the benchmark data. Ghia *et al.* [16] adopted quite a fine grid of 129×129 in their computation. However, it is found that when the grid is as fine as 71×71, the present predictions are in good agreement with the benchmark data. Computed streamlines in the 90° cavity are plotted in Figure 4. It is easily observed that the profiles of the streamlines are quite reasonable when compared with those of Ghia *et al.* [16]. It should be noted that in the following computations, a moderate uniform grid of 35×35 is used, and the convergence criterion is that the maximum residuals in all equations fall below 10^{-6} so as to save computer time.

Computed streamlines in the cavity at $\beta = 60°$ by the Cartesian and covariant velocity methods are plotted in Figure 5(a) and (b) respectively. It is observed that the computed streamlines by the Cartesian velocity method are nearly identical to those by the covariant velocity method. Computed streamlines in the cavity at $\beta = 45°$ and 30° are shown in Figures 6 and 7 respectively. It is also found that the streamline profiles by the Cartesian and covariant velocity methods are almost identical to each other. Therefore, it may be concluded that regardless whether the Cartesian velocity components or the covariant velocity components are adopted as the main variables in the momentum equations, the numerical accuracy is the same.

3.2. Convergence

The convergence performance of the SIMPLEC method for the 90° cavity flow with a Reynolds number of 100 is shown in Figure 8. It is found that when α_p is larger than 0.5, the iteration number needed to get a convergent solution does not change very much. This is because the pressure–velocity coupling is easier to carry out on an orthogonal grid. With the increase of α_u, the iteration number required decreases.

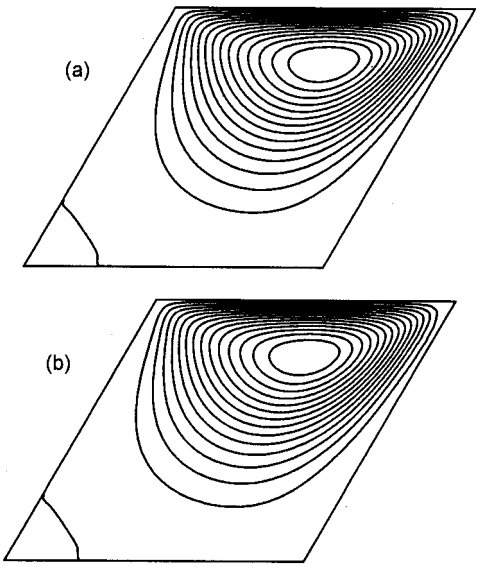

Figure 5. Calculated streamlines for a cavity at $\beta = 60°$, $Re = 100$: (a) Cartesian velocity method; (b) covariant velocity method.

The convergence performance of the Cartesian and covariant velocity methods for the cavity flow at $\beta = 60°$ is shown in Figure 9 with various α_u. It is found that when $\alpha_p < 0.8$, the iteration numbers in the two methods are close to each other. However, the iteration numbers by the covariant velocity method are somewhat less than those by the Cartesian velocity method. From Figures 9(a) and (b), it is seen that when $\alpha_p > 0.8$, the iteration numbers in the covariant velocity method increase, while the iteration numbers in the Cartesian velocity method decrease.

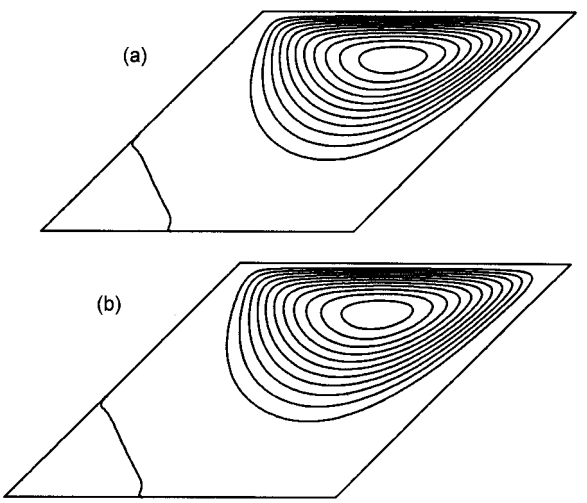

Figure 6. Calculated streamlines for a cavity at $\beta = 45°$, $Re = 100$: (a) Cartesian velocity method; (b) covariant velocity method.

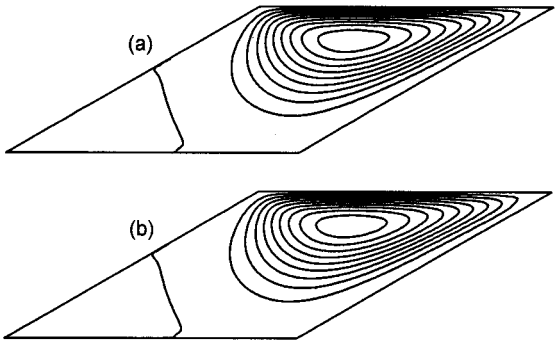

Figure 7. Calculated streamlines for a cavity at $\beta = 30°$, $Re = 100$: (a) Cartesian velocity method; (b) covariant velocity method.

The corresponding convergence performance of the two methods for the case of $\beta = 45°$ is shown in Figure 10. For cases of $\alpha_u = 0.5$ and 0.6, when $\alpha_p < 0.5$, the iteration numbers by the covariant velocity method are less than those by the Cartesian velocity method. However, when $\alpha_p > 0.5$, the iteration numbers required by the covariant velocity method increase rapidly. For cases of $\alpha_u = 0.7$ and 0.8, a similar conclusion can be drawn from Figure 10(c) and (d).

The convergence performance of the two methods for the case of $\beta = 30°$ is plotted in Figure 11. It is easily found that when α_p is very small (around 0.3), the iteration numbers required by the covariant velocity method are less than those required by the Cartesian velocity method. Unfortunately, when α_p increases, the iteration numbers required by the covariant velocity method do not decrease as the Cartesian velocity method, but increase inversely. The convergence range of α_p in the covariant velocity method is very narrow, while in the Cartesian velocity method, the convergence range of α_p is quite wide. This is the main difference between the two methods.

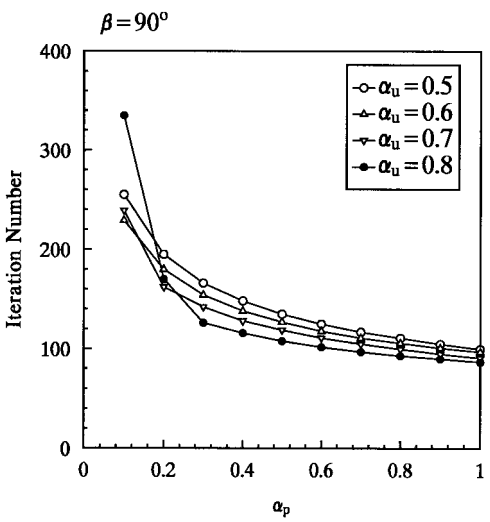

Figure 8. Convergence performance for a cavity at $\beta = 90°$, $Re = 100$.

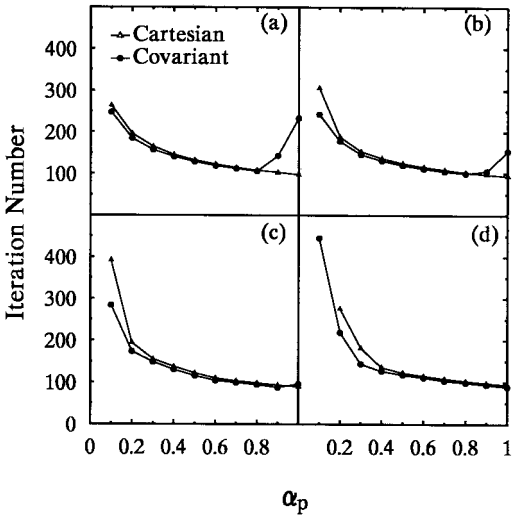

Figure 9. Convergence performance of the two methods for a cavity at $\beta = 60°$, $Re = 100$: (a) $\alpha_u = 0.5$, (b) $\alpha_u = 0.6$, (c) $\alpha_u = 0.7$ and (d) $\alpha_u = 0.8$.

From the above comparisons, it may be concluded that for cases of $\beta \geq 60°$, the convergence performance of the Cartesian and covariant velocity methods is not so different from each other. However, for cases of $\beta \leq 45°$, the convergence performance of the two methods is completely different from each other. When α_p is quite small, the iteration numbers by the covariant velocity method are less than those by the Cartesian velocity method. When α_p increases, the iteration numbers by the covariant velocity method will increase rather than decrease, as for the Cartesian velocity method. For most cases, it is hard to get a convergent solution by the covariant velocity method unless α_p is very small. Therefore, the convergence range of α_p in the covariant velocity method becomes very narrow when β is small. For the

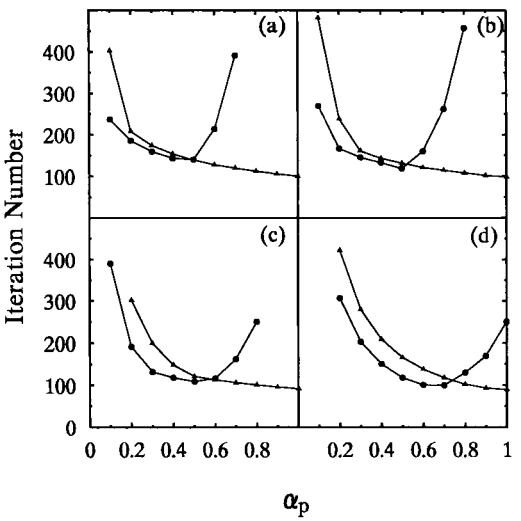

Figure 10. Convergence performance of the two methods for a cavity at $\beta = 45°$, $Re = 100$: (a) $\alpha_u = 0.5$, (b) $\alpha_u = 0.6$, (c) $\alpha_u = 0.7$ and (d) $\alpha_u = 0.8$. Notations as in Figure 9.

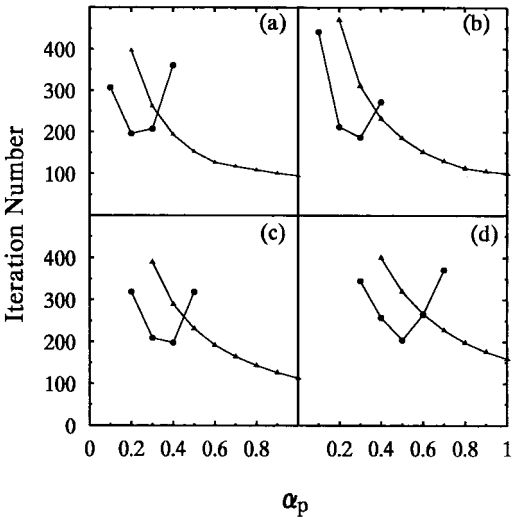

Figure 11. Convergence performance of the two methods for a cavity at $\beta = 30°$, $Re = 100$: (a) $\alpha_u = 0.5$, (b) $\alpha_u = 0.6$, (c) $\alpha_u = 0.7$ and (d) $\alpha_u = 0.8$. Notations as in Figure 9.

Cartesian velocity method, a convergent solution can be obtained when α_p becomes as large as unity, and β is as small as 30°. When α_p is very small, the covariant velocity method is faster than the Cartesian velocity method. However, the overall performance of the Cartesian velocity method should be superior to that of the covariant velocity method.

In order to examine the influence of the Reynolds number on the convergence rates, the 30° cavity flow at $Re = 1000$ is also calculated by both methods using the same grid number as for the case of $Re = 100$. The convergence performance is shown in Figure 12. It is found that the convergence performances of the Cartesian and covariant methods are similar to those for the 30° cavity flow at $Re = 100$. From the comparison between Figures 11 and 12, it is seen that

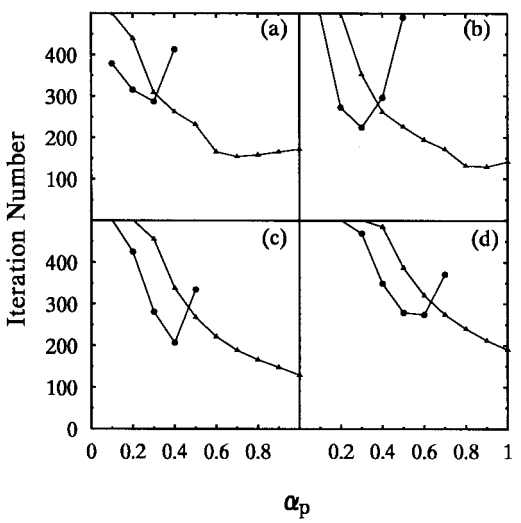

Figure 12. Convergence performance of the two methods for a cavity at $\beta = 30°$, $Re = 1000$: (a) $\alpha_u = 0.5$, (b) $\alpha_u = 0.6$, (c) $\alpha_u = 0.7$ and (d) $\alpha_u = 0.8$. Notations as in Figure 9.

the convergence rate for both methods decreases with increasing Reynolds number. To get a higher Reynolds number, the viscosity of fluid should decrease if the velocity of the moving lid is kept constant. Therefore, it will become slower to transfer the boundary information to the interior region of the cavity during the numerical iteration. This is the reason why the convergence rate for higher Reynolds number flow will decrease.

3.3. Discussions

From the above comparisons, it is concluded that the overall convergence performance of the Cartesian velocity method is better than that of the covariant velocity method. This is not consistent with the usual idea that the adoption of the covariant velocity method should be better than that of the Cartesian velocity method. This is discussed below.

When the pressure-correction equation is formulated, the cross-derivatives of the pressure corrections in Equations (20a) and (20b) are usually neglected to avoid solving a nine-diagonal matrix. Due to the omission of the cross-derivatives of the pressure corrections, it is not so proper to correct the covariant velocity components using Equations (21a) and (21b) in the covariant velocity method after the pressure-correction equation has been solved.

In order to consider the effect of the cross-derivatives of the pressure corrections, Wang and Komori (1998, submitted) treated the cross-derivatives approximately. For example, p'_η in Equation (20a) at point e can be calculated by

$$p'_{\eta,\mathrm{e}} = \frac{p'_{\mathrm{ne}} - p'_{\mathrm{se}}}{(\delta\eta)_P} \approx \frac{p'_{\mathrm{n}} - p'_{\mathrm{s}}}{(\delta\eta)_P} \approx \frac{p'_{\mathrm{N}} - p'_{\mathrm{S}}}{(\delta\eta)_{\mathrm{n}} + (\delta\eta)_{\mathrm{s}}}. \tag{32a}$$

Similarly, p'_ξ in Equation (20b) at point n can be calculated according to

$$p'_{\xi,\mathrm{n}} = \frac{p'_{\mathrm{ne}} - p'_{\mathrm{nw}}}{(\delta\xi)_P} \approx \frac{p'_{\mathrm{e}} - p'_{\mathrm{w}}}{(\delta\xi)_P} \approx \frac{p'_{\mathrm{E}} - p'_{\mathrm{W}}}{(\delta\xi)_{\mathrm{e}} + (\delta\xi)_{\mathrm{w}}}. \tag{32b}$$

When this approximate treatment for the cross-derivatives is used, the coefficients in Equation (26) can be rewritten as

$$A^p_{\mathrm{E}} = (\rho B\Delta\eta/\delta\xi)_{\mathrm{e}} + \underline{[(\rho E\Delta\xi)_{\mathrm{n}} - (\rho E\Delta\xi)_{\mathrm{s}}]/[(\delta\xi)_{\mathrm{e}} + (\delta\xi)_{\mathrm{w}}]}, \tag{33a}$$

$$A^p_{\mathrm{W}} = (\rho B\Delta\eta/\delta\xi)_{\mathrm{w}} - \underline{[(\rho E\Delta\xi)_{\mathrm{n}} - (\rho E\Delta\xi)_{\mathrm{s}}]/[(\delta\xi)_{\mathrm{e}} + (\delta\xi)_{\mathrm{w}}]}, \tag{33b}$$

$$A^p_{\mathrm{N}} = (\rho C\Delta\xi/\delta\eta)_{\mathrm{n}} + \underline{[(\rho D\Delta\eta)_{\mathrm{e}} - (\rho D\Delta\eta)_{\mathrm{w}}]/[(\delta\eta)_{\mathrm{n}} + (\delta\eta)_{\mathrm{s}}]}, \tag{33c}$$

$$A^p_{\mathrm{S}} = (\rho C\Delta\xi/\delta\eta)_{\mathrm{s}} - \underline{[(\rho D\Delta\eta)_{\mathrm{e}} - (\rho D\Delta\eta)_{\mathrm{w}}]/[(\delta\eta)_{\mathrm{n}} + (\delta\eta)_{\mathrm{s}}]}. \tag{33d}$$

The underlined parts in Equations (33a)–(33d) are the contributions of the cross-derivatives of the pressure corrections. It should be noted that A^p_P and m_p in Equation (26) remain unchanged. Here the modification is just referred to as the modified form of the covariant velocity method.

Comparisons of the convergence performance of the covariant velocity method and its modified form are shown in Figure 13. It is found that for cases of $\beta = 30°$ and 45°, the convergence performance of the modified form becomes much better than that of its original form. For the case of $\beta = 60°$, the improvement is not so significant since the cross-derivatives of the pressure corrections are not so important. Therefore, in order to get the better convergence performance on strongly non-orthogonal grids, it is quite necessary to consider the cross-derivatives of the pressure corrections.

In the SIMPLE-like method, the relaxation factor for pressure, α_p, is one of the most important parameters. The choice of a proper α_p is the precondition to get a convergent

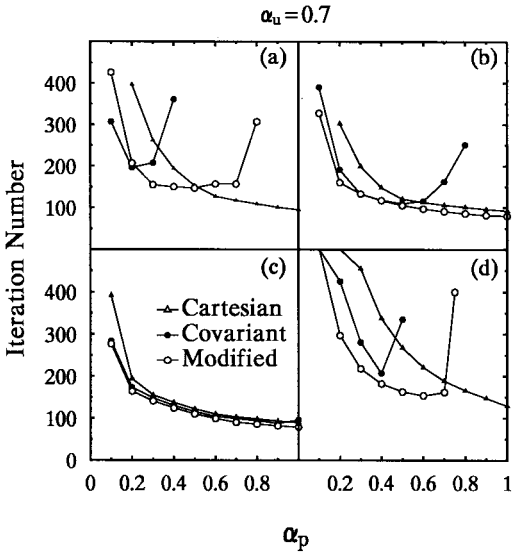

Figure 13. Convergence performance comparisons for a cavity at (a) $\beta = 30°$, $Re = 100$; (b) $\beta = 45°$, $Re = 100$; (c) $\beta = 60°$, $Re = 100$; (d) $\beta = 30°$, $Re = 1000$.

solution. For an orthogonal grid, an underrelaxation factor of 0.8 for α_p is usually recommended in the SIMPLE method [2], since terms like $\Sigma A_{nb} u'_{nb}$ and $\Sigma A_{nb} v'_{nb}$ in Equations (17a) and (17b) are omitted in the derivation of the pressure-correction equation. In the SIMPLEC method, however, terms like $\Sigma A_{nb}(u'_{nb} - u'_p)$ and $\Sigma A_{nb}(v'_{nb} - v'_p)$ are omitted [3]. The omission in the SIMPLEC method is more reasonable than in the SIMPLE method, therefore, a relaxation factor as high as unity can be adopted for α_p. For non-orthogonal grids, Peric [9] derived a formulation between the optimum relaxation factor for pressure and that for velocity as $\alpha_p = 1.1 - \alpha_u$ in the SIMPLE method. From the present calculated results using the SIMPLEC method, it is found that the optimum value for α_p is also unity when the Cartesian method is used. When the covariant method is used, however, the optimum value for α_p may depend on the skew angle of the cavity. For $\beta = 60°$ the optimum value for α_p is 0.8. For $\beta = 45°$, the optimum value for α_p is around 0.5. For $\beta = 30°$, the optimum value for α_p is around 0.4. Therefore, a safer relaxation factor of 0.4 for α_p can be adopted for strongly non-orthogonal grids. When the cross-derivatives of the pressure corrections are considered, a safer relaxation factor as high as 0.7 can be used for very strongly non-orthogonal grids. Therefore, the inclusion of the cross-derivatives of the pressure corrections is very successful.

4. CONCLUDING REMARKS

On non-orthogonal collocated grids, the Cartesian and covariant velocity methods are used to calculate a two-dimensional lid-driven cavity flow. Numerical accuracy and convergence performance of the two methods are compared from the results of a large number of computer computations. Comparisons show that both the Cartesian and covariant velocity methods have the same numerical accuracy for the same cavity flow. The convergence rate of the covariant velocity method is faster than that of the Cartesian velocity method when α_p is quite small. However, the convergence range of the relaxation factor α_p in the covariant velocity method is

fairly narrow. When the cross-derivatives in the pressure-correction equation are treated approximately, the convergence performance of the covariant velocity method can be greatly improved. Therefore, the treatment of the cross-derivatives in the pressure-correction equation is quite important in computing fluid flows on strongly non-orthogonal grids.

REFERENCES

1. S.V. Patankar and D.B. Spalding, 'A calculation procedure for heat, mass and momentum transfer in three-dimensional parabolic flows', *Int. J. Heat Mass Transfer*, **15**, 1787–1806 (1972).
2. S.V. Patankar, *Numerical Heat Transfer and Fluid Flow*, Hemisphere, Washington, DC, 1980.
3. J.P. Van Doormaal and F.D. Raithby, 'Enhancements of the SIMPLE method for predicting incompressible fluid flows', *Numer. Heat Transf.*, **7**, 147–163 (1984).
4. C.M. Rhie and W.L. Chow, 'Numerical study of the turbulent flow past an airfoil with trailing edge separation', *AIAA J.*, **21**, 1525–1532 (1983).
5. M. Peric, R. Kessler and F. Scheuerer, 'Comparison of finite volume numerical methods with staggered and collocated grids', *Comput. Fluids*, **16**, 389–403 (1988).
6. M.C. Melaaen, 'Calculation of fluid flows with staggered and non-staggered curvilinear non-orthogonal grids—the theory', *Numer. Heat Transf. B*, **21**, 1–19 (1992).
7. M.C. Melaaen, 'Calculation of fluid flows with staggered and non-staggered curvilinear non-orthogonal grids—a comparison', *Numer. Heat Transf. B*, **21**, 21–39 (1992).
8. L. Davidson and P. Hedberg, 'Mathematical derivation of a finite volume formulation for laminar flow in complex geometries', *Int. J. Numer. Methods Fluids*, **9**, 531–540 (1989).
9. M. Peric, 'Analysis of pressure–velocity coupling on non-orthogonal grids', *Numer. Heat Transf. B*, **17**, 63–82 (1990).
10. J. Rincon and R. Elder, 'A high-resolution pressure-based method for compressible flows', *Comput. Fluids*, **26**, 217–231 (1997).
11. K.C. Karki and S.V. Patankar, 'Calculation procedure for viscous incompressible flows in complex geometries', *Numer. Heat Transf.*, **14**, 295–307 (1988).
12. I. Demirdzic, Z. Lielk and M. Peric, 'A collocated finite volume method for predicting flows at all speeds', *Int. J. Numer. Methods Fluids*, **16**, 1029–1050 (1993).
13. P. Tamamidis and D.N. Assanis, 'Prediction of three-dimensional steady incompressible flows using body-fitted co-ordinates', *ASME J. Fluids Eng.*, **115**, 457–462 (1993).
14. Y. Wang and S. Komori, 'Prediction of duct flows with a pressure-based procedure', *Numer. Heat Transf. A*, **33**, 723–748 (1998).
15. S. Majumdar, 'Role of underrelaxation in momentum interpolation for calculation of flow with nonstaggered grids', *Numer. Heat Transf.*, **13**, 125–132 (1988).
16. U. Ghia, K.N. Ghia and C.T. Shin, 'High-resolutions for incompressible flow using the Navier–Stokes equations and a multigrid method', *J. Comput. Phys.*, **48**, 387–411 (1982).

